International Journal of Architectural, Civil and Construction Sciences
ISSN: 2415-1734
Vol:13, No:6, 2019

Simplified 3R2C Building Thermal Network Model: A Case Study

S. M. Mahbobur Rahman

***Abstract*—**Whole building energy simulation models are widely used for predicting future energy consumption, performance diagnosis and optimum control. Black box building energy modeling approach has been heavily studied in the past decade. The thermal response of a building can also be modeled using a network of interconnected resistors (R) and capacitors (C) at each node called R-C network. In this study, a model building, Case 600, as described in the "Standard Method of Test for the Evaluation of Building Energy Analysis Computer Program", ASHRAE standard 140, is studied along with a 3R2C thermal network model and the ASHRAE clear sky solar radiation model. Although building an energy model involves two important parts of building component i.e., the envelope and internal mass, the effect of building internal mass is not considered in this study. All the characteristic parameters of the building envelope are evaluated as on Case 600. Finally, monthly building energy consumption from the thermal network model is compared with a simple-box energy model within reasonable accuracy. From the results, 0.6-9.4% variation of monthly energy consumption is observed because of the south-facing windows.

***Keywords*—**ASHRAE case study, clear sky solar radiation model, energy modeling, thermal network model.

I. Introduction

BUILDINGS account for 36% of total energy usage and 65% of total electricity consumption in the USA according to the United States Green Building Council [1]. According to some studies, energy consumption share is even higher, 39% of total energy usage in the US and 40% of total energy consumption in Europe [2], [4], [5]. The energy usage, generated from fossil fuel, contributes to CO_2 emission, causing air pollution and global warming. Besides escalating energy usage trend, buildings also contribute towards 38% of the CO_2 emission in the US and 36% of the same in Europe [5]. Limited availability of energy and the highly transient nature of renewable energy sources have furthered the prominence of energy efficiency and conservation in various sectors. Energy consumption of buildings increases marginally by 138MW due to 1^{o}C outdoor air dry-bulb temperature in South Africa [14]. Scientists warn that energy consumption may soar by 28% by 2035 [2].

Previously, building a thermal network model was used for temperature regulation. Active management of room temperature set points can save up to 20% energy cost and substantial savings, up to 30%, through doors and windows opening and closing at a certain time - two important findings of the study conducted by Qi Luo and Ariyur Kartik [6]. The building 3R2C thermal network model was also utilized in combination with Genetic Algorithm (GA) for dynamic building energy simulation, combining both the building envelope and internal mass by Xinhua Xu and Shengwei Wang [7]. One important finding from their study was that higher order thermal network models should be used for heavy weighted constructions when simplifying the model if higher accuracy is a concern. Reference [8] used a model based approach to estimate zonal loads in a commercial building and found that real-time solar data provides better estimation than simulated data. A GA-based parameter identification and 3R2C thermal network model in combination with a simplified internal mass model and an internal cooling load model based on submetering data were utilized for a commercial building with good accuracy [11]. Reference [13] utilized four thermal network models, namely 1R1C, 3R2C, 4R2C, and 8R3C, on an occupied building measured data and concluded that higher order models performed better in their case. Their models were used to successfully predict the indoor air temperature of an occupied office building. Data driven identification of an R-C network was used in the US for a 5-zone office building which could successfully reconstruct the interaction topology of an EnergyPlus model [15]. Their proposed learning algorithm reconstructs the interaction topology more precisely if more and more samples were used for learning.

In this study, a model building, Case 600 as described in "Standard Method of Test for the Evaluation of Building Energy Analysis Computer Program", ASHRAE standard 140, 2007, is evaluated. To estimate the building annual heating and cooling load using simplified building energy model, outdoor air temperature and humidity, indoor air temperature and humidity, fresh air flow rate, solar radiation, occupancy and internal gains are required. The model, obtained through convective and conductive heat transfer between building envelope and the surroundings, relates the environmental conditions of a building to its heating and cooling loads. Apart from weather conditions and occupancy load, lighting load and equipment load, the physical property of the building also greatly affect the heating and cooling energy consumption. The physical property of a building includes building envelopes, such as walls, roofs, and building internal mass, includes interior wall, floor, partition, carpet, and furniture etc. The building is modeled as a thermal network; a passive circuit with room heaters as heat sources and the ambient environment as the heat sink. In this study, the effect of humidity, occupancy, infiltration, and building internal mass on building energy consumption is ignored, however.

S. M. Mahbobur Rahman was with the University of Texas at San Antonio, San Antonio, TX 78249 USA. He is now with Pristine Engineers, Inc, Raynham, MA 02767 USA (e-mail: pew6555@ my.utsa.edu).

II. Modeling Approach

Researchers in this arena have classified building energy modeling approaches into three broad and distinct categories i.e., white box, black box, and grey box modeling [2], [4].

White box modeling approach is widely utilized in the industry to get information about a whole building and their sub-system behavior, including energy consumption, thermal comfort condition, lighting intensity, etc. Utilizing a detailed physics-based equation to capture the building dynamics, white box models can provide precise estimates of the whole building energy consumption. The simulation engine will run the series of mathematical equations to simulate the building operation and calculate the energy consumption. Detailed heat balance calculations are carried out at discrete time steps based on the physical properties of the building and mechanical systems along with dynamic external inputs. Most common software tools to utilize white box models are DOE-2, EnergyPlus, TRNSYS, ESP-r. Commercially available white box modeling tools, such as Trane Trace 700, Carrier HAP, DesignBuilder etc., provide more flexibility, along with utility rate structure, to automate cost savings calculation over the course of time. Reference [16] outlines a comparison of the main features and capabilities of the top 20 tools commonly utilized for the white box modeling approach. The whole building energy modeling approach, required for the Leadership in Energy and Environmental Design (LEED) rating system, developed by the US Green Building Council (USGBC), utilizes this technique. White box modeling approach is also known as forward modeling approach, engineering methods or physics based methods.

Black box modeling approach, also known as data-driven approach, utilizes historical building energy consumption data, measured or simulated, to feed machine learning or statistical models, such as Artificial Neural Network, Support Vector Machine, Gaussian Process Regression etc., to forecast the energy consumption without considering building envelope and internal mass parameters [14], [18]. Most research in the building energy domain has been conducted using back box modeling approach in the past decade [3].

Gray box modeling or hybrid modeling approach formulates a physical model to represent the building envelope or internal mass and then identifies model parameters using statistical analysis or black box modeling approach. These types of models are claimed to have higher accuracy among the three approaches [3], [18], [19].

Reference [3] tabulated the comparative positive and negative aspects of the above three approaches.

III. Building Geometry

The base building plan is a single story, unshaded, low mass building with rectangular-prism geometry, 48 m^2 floor area. It also has two south facing double pan windows, 6 m^2 area each, with 1 m gap between them. The building wall, roof and floor thickness are defined in such a way that the internal volume of the building remains same, 129.6 m^3. Although heat loss to the ground can have a significant impact on the building energy consumption, the state-of-the-art in ground modeling is not very good even in detailed building energy simulation programs. To reduce uncertainty, the floor insulation has been made very thick to effectively decouple the floor thermally from the ground.

The building has an internally generated sensible heat gain of 200 W for 24 hours of the day for the full year. Thermal resistance of the wall and environment changes significantly when doors or windows are closed or opened. These effects are not considered in this study. Although cooling load calculation has two components, only sensible cooling is considered in this study.

For this study, Typical Meteorological Year (TMY) data, such as, outdoor air dry-bulb temperature, direct normal radiation and diffused horizontal radiation, were used for the site, longitude and latitude are 39.76 and -104.86, respectively, located in Denver, Colorado, USA of the year 1969. Material properties, evaluated from the corresponding tables of Case 600 and TMY historical data are used to build and simulate the mathematical model in the MATLAB, computational software tool.

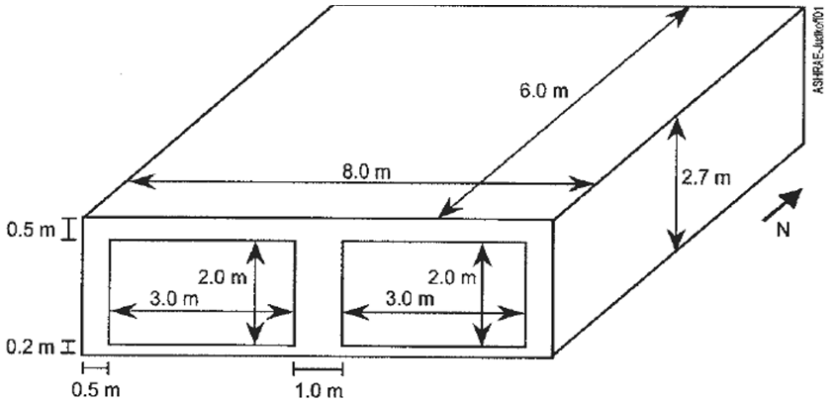

Fig. 1 Building prototype (Case 600)

IV. Clear Sky Solar Radiation Model

Clear sky solar radiation varies significantly at different times of the day and of the year. Solar radiation has significant impact on building envelope and internal mass [1], [18], [19], [9]. Therefore, building heating and cooling load also vary based on the position of the sun, as we get different radiance from the sun on different sides of the building geometry at different times of the day. A profound comprehension on solar time and Earth time is required to take into account this variation as they are highly seasonal around the year. It is important to note that on Earth, we have several time zones. This section is dedicated for the modeling of variation between solar time and Earth time and also the radiation we will get from the sun due to the variation of its position. It is noteworthy that, angles, in all equations in this section, are expressed in degrees including the arguments appearing in trigonometric functions.

The Earth orbits around the sun and completes its journey every 365 mean solar days. The Earth's orbital velocity, which is responsible for the apparent movement of the sun as it appears from Earth, also varies throughout the year. Hence, Apparent Solar Time (AST) also varies with the mean time as we see in a clock on Earth. This variation is approximated by Equation of Time (ET), which is best approximated by (1). Equation (1), empirical, corrects the eccentricity of Earth's orbit and axial tilt.

$$\mathrm{ET} = 2.2918 \times (0.0075 + 0.1868 \times \mathrm{Cos}(\Gamma) - 3.2077 \times \mathrm{Sin}(\Gamma) - 1.4615 \times \mathrm{Cos}(2\Gamma) - 4.089 \times \mathrm{Sin}(2\Gamma) \quad (1)$$

$$\Gamma = 360^{o} \times \frac{\mathrm{n}-1}{365} \quad (2)$$

where, n is the day of the year (1 for Jan 31, 32 for Feb 1). Standard Meridian Longitude (LSM) is related to the Time Zone (TZ) based on following equation:

$$\mathrm{LSM} = 15 \times \mathrm{TZ} \quad (3)$$

where, TZ is evaluated from corresponding table of ASHRAE climate design conditions, found in ASHRAE handbook fundamentals [10].

Finally, ET is added to the Local Standard Time (LST) and a longitude correction factor is applied to get the Apparent Solar Time (AST). This longitude correction takes into account the variation of site time with respect to the respective time zone on Earth, which is four minutes of time per degree difference between the Local Site Longitude (LON) and longitude of the Local Standard Meridian (LSM). Local Time (LT) usually varies from LST because of the eccentricity of Earth's orbit, and also, because of human adjustments such as time zones and daylight saving. AST can be best approximated by (4).

$$AST = LST + \frac{ET}{60} + \frac{(LON-LSM)}{15} \quad (4)$$

In this study, variation of the Local Standard Time (LST) due to the Daylight Saving Time (DST) is not considered because the effect would be negligible for a building of comparatively smaller footprint.

The declination angle, δ, varies seasonally due to the tilt of the earth on its axis of rotation and its rotation around the sun. Earth's equatorial plane is tilted at an angle of 23.45° to the orbital plane; hence, solar declination angle is used to encounter the variation of changing seasons with their unequal daylight time and unequal darkness time based on (5).

$$\delta = 23.45 \times \mathrm{Sin}(360^{o} \times \frac{\mathrm{n}+284}{365}) \quad (5)$$

The hour angle, H, variation is a function of apparent solar time, defined as the angular displacement of the sun east or west of the local meridian due to the rotation of the earth. It converts the LST into the number of degrees, which the sun moves across the sky. The hour angle is 0° at solar noon, when the sun reaches its maximum altitude in the sky, positive in the afternoon and negative in the morning, by definition. The hour angle, between solar noon and instantaneous location of the sun, changes by 15° each hour because the earth rotates 15° each hour. The hour angle can be estimated from (6).

$$H = 15 \times (AST - 12) \quad (6)$$

The solar attitude angle, β, changes with local longitude, solar declination and hour angle. The variation among them is best encountered based on (7).

$$Sin(\beta) = Cos(L) \times Cos(\delta) \times \mathrm{Cos(H)} + \mathrm{Sin(L)} \times \mathrm{Sin}(\delta) \quad (7)$$

The compass direction of the coming sunlight is defined by the azimuth angle, ϕ. The sun is always directly north and directly south at solar noon in the southern and northern hemispheres, respectively. In general, the azimuth angle varies with the latitude and time of year, and the equations to calculate the sun's position throughout the day are given by (8).

$$Sin(\phi) = Sin(H) \times \frac{Cos(\delta)}{Cos(\beta)} \quad (8)$$

Solar radiation at the earth's surface varies significantly because of the property of the surface even though actual incident solar radiation on the earth's atmosphere is relatively constant. Major issues impacting received solar radiation at the earth's surface are: 1) atmospheric effects i.e., absorption, scattering, 2) atmospheric component i.e., water vapor, clouds, and pollution variation, 3) geographic latitude, and 4) seasonal variation and daily time variation. These issues play a significant role in the overall power received from the sun, light spectral content and the light incident angle on a surface. Variation of the amount and location of the clouds as well as seasons on Earth, as well as day length at a particular geographic location etc., also contribute toward the solar radiation incident on the earth's surface.

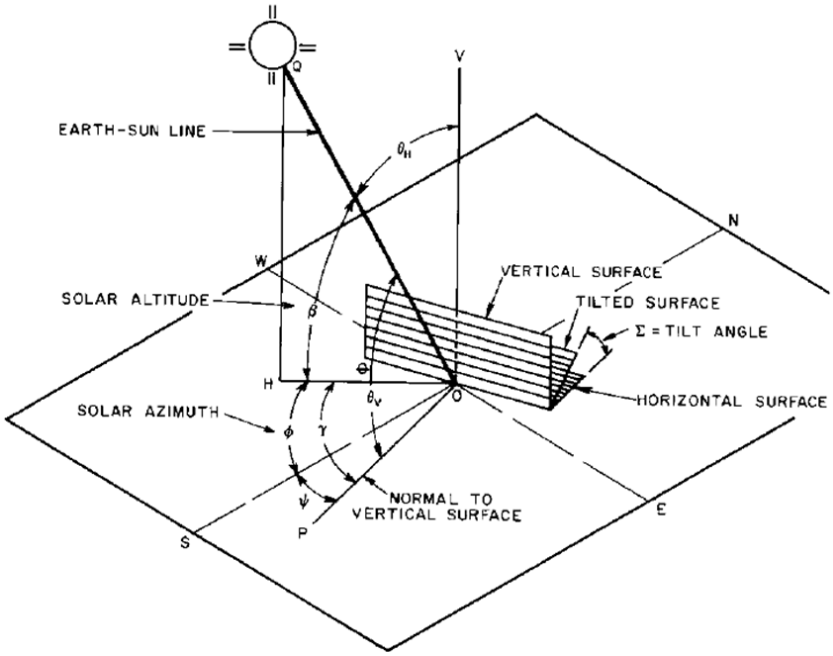

Fig. 2 Solar angles for vertical and horizontal surfaces [10]

The surface-solar azimuth angle, γ, is defined as the angular difference between the solar azimuth, ϕ, and the surface azimuth, ψ.

$$\gamma = \phi - \psi \tag{9}$$

Angle of inclination, θ, affects the intensity of the direct component of the solar radiation striking the surface and the surface's ability to absorb, transmit or reflect the Sun's rays. The angle of inclination is best approximated by (10) for vertical surface and by (11) for horizontal surface.

$$\text{Cos}\,(\theta) = \text{Cos}(\beta) \times \text{Cos}(\gamma) \tag{10}$$

$$\theta = 90^{o} - \beta \tag{11}$$

Total clear-sky irradiance, Et, reaching the receiving surface is the sum of three components: the beam component, Et,b, originating from the solar disc; the diffuse component, Et,d, originating from the sky dome; and the ground-reflected component, Et,r, originating from the ground in front of the receiving surface.

$$\text{Et} = \text{Et,b} + \text{Et,d} + \text{Et,r} \tag{12}$$

The beam component calculation is a straight forward geometric problem.

$$\text{Et,b} = \text{Eb} \times \text{Cos}(\theta) \tag{13}$$

This relationship is valid only for positive values of Cos(θ), otherwise the value of Et,b is taken as zero.

Since the diffused component of solar radiation is non-isotropic, estimating the diffused component is more challenging than the simple beam component. Circumsolar disc or the horizon, along with other parts of the sky, is comparatively brighter than other parts, which is also the reason why development of a simplified model is difficult. If Y is the ratio of clear-sky diffuser radiation on a vertical surface to clear-sky diffuser irradiance on the horizontal surface, it is estimated that Y can be expressed as a function of θ, the angle of incidence, which is given by (14).

$$\text{Et,d} = \text{Ed} \times \text{Y} \tag{14}$$

$$Y = max(0.45, 0.55 + 0.437 \times Cos(\theta) + 0.313\, Cos^{2}(\theta))$$

In our model geometry of Case 600, south-side double window, having area of 6 m^2 each, is modeled as a single equivalent window with a 12 m^2 area. Window transmissivity is found from a corresponding table of the Case 600. As the transmissivity is dependent on angle on inclination, we formulated a fourth order equation to calculate the transmissivity at different angles. This equation, (15), is derived from the angle of incidence and transmissivity relationship as described in corresponding table of Case 600.

$$\text{Window transmissivity} = -0.000000046853146853 1371 \times \theta^{4} + 0.000004415695415696 18 \times \theta^{3} - 0.000146486013986258 \times \theta^{2} + 0.0014116355866598 \times \theta + 0.746149184148711 \tag{15}$$

Ground reflected component, Et,r, is neglected for this study.

Exterior surface solar distribution is calculated based on opaque surface radiative properties as tabulated in Case 600. Interior solar distribution fraction is calculated for each and

every surface and roof, based on the interior solar distribution fractions as tabulated in the reference table of Case 600.

V. Thermal Model

A simplified 3R2C network is used for the thermal model evaluation. In the 3R2C thermal network model, the three R's are the exterior surface combined convective and radiative heat transfer resistance, wall thermal conductive resistance and the internal zone convective and radiative heat transfer resistance, and two C's are the wall capacitance and zonal node capacitance. Eleven nodes were used for the whole building envelope thermal modeling. Each wall consists of two nodes and the wall node capacitance values are evaluated as half of the corresponding wall capacitance.

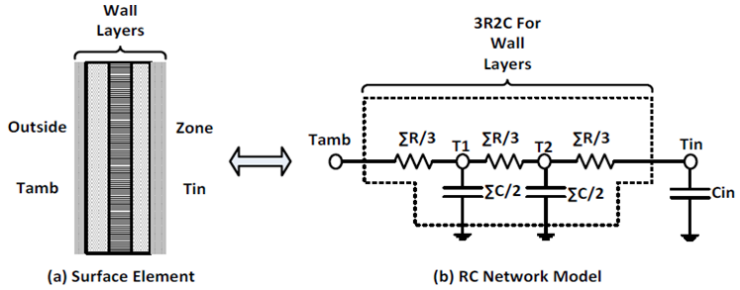

Fig. 3 Simplified 3R2C thermal network model for the wall [1]

A schematic of the wall and roof molding procedure is outlined in Fig. 3. In this case study, we added an equivalent parallel resistance from outside ambient to zone for modeling the window on south side of the Case 600 model building.

$$C_2 \frac{dT_1}{dx} = \frac{T_{amb}-T_1}{R_1} + \frac{T_2-T_1}{R_3} + Q_{outside\_absorbed\_solar\_irradiance} \quad (16)$$

$$C_4 \frac{dT_1}{dx} = \frac{T_1-T_2}{R_3} + \frac{T_{in}-T_2}{R_5} + Q_{inside\_absorbed\_solar\_irradiance} \quad (17)$$

Refer to (18) to obtain sensible heat balance for the zone. In our study, the effect of adjoined zones is ignored since there are no adjoined zones in Case 600. Infiltration mass is considered to be 0.5 of air change per hour (ACH).

$$m_{air\_zone} C_{pa} \frac{dT_{zone}}{dt} = \dot{m}_{air\_sa} C_{pa} (T_{sa} - T_{zone}) + Q_{int} + \sum_i^{N_{surface}} Q_{structure\_i} + \dot{m}_{inf} C_{pa} (T_{oa} - T_{zone}) + \sum_i^{N_{surface}} \dot{m}_i C_{pa} (T_{adjzonei} - T_{zone}) + Q_{structure} = h_i A (T_{isuf} - T_{zone}) + \frac{T_{amb}-T_{zone}}{R_{win}} \quad (18)$$

where, m_{air_zone}= zone air mass, C_{pa}= outdoor equivalent air specific heat, Q_{int}= internal heat gain, $Q_{structure}$= heat gain from the walls, $\dot{m}_{inf}$= infiltration mass flow rate, T_{oa}= temperature of outdoor air.

Equivalent heat transfer coefficient connectivity matrix was formulated with the 11 ODE's for the 11 nodes in the geometry. Then, the system of differential equations was solved in MATLAB using ODE solvers.

VI. Results

For result evaluation, the following thermostat control strategy is followed from ASHRAE standard 90.1:

Heating=ON; while zone temperature ≤ 21.11°C
Heating=OFF; while zone temperate > 21.11°C
Cooling=ON; while zone temperature ≥ 23.89°C
Cooling=OFF; while zone temperature < 23.89°C

When the conditioned zone temperature exceeds thermostat cooling set point, the heat extraction rate is assumed to be equal to the maximum capacity of the cooling element. Similarly, when the conditioned zone temperature drops below the thermostat heating set point, the heat addition rate is assumed to be equal to the maximum capacity of the heating element.

TMY weather data for Denver, Colorado, USA, is used for this case study. It is important to note that, TMY weather data represents average weather patterns over the course of a significant period of time in the past, because no single year weather data can represent the long-term weather pattern for a particular region. Denver is typically in a cold region, having its highest temperature of 35°C in July and lowest temperature of -24.4°C observed in January for the year of 1969. Fig. 4 illustrates the annual hourly outdoor air-dry bulb temperature distribution for Denver, along with the heating and cooling thermostatic setpoints. From Fig. 4, we can expect significant heating load and comparatively lower cooling load over the course of the year in Denver, since most of the time, the temperatures are below 21.11°C, our heating setpoint.

We also created a "simple-box" energy model, using similar parameters in eQuest to compare our model with the equivalent energy modeling tool. Based on our heating and cooling setpoints and outdoor air temperature distribution, the number of hours of heating or cooling energy that will be required are tabulated in Table I.

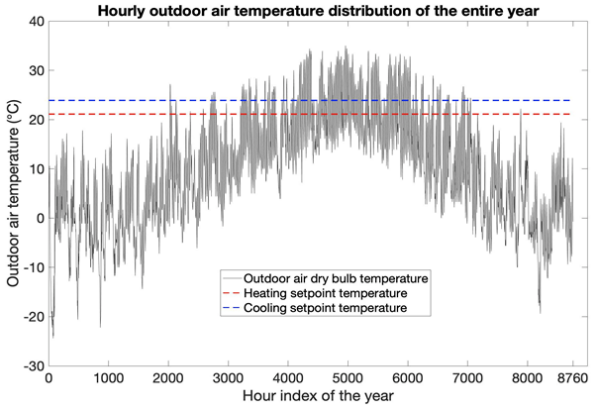

Fig. 4 Hourly outdoor air temperature distribution for the entire year

TABLE I
ANNUAL HOURLY LOAD DISTRIBUTION

Month	Hours heating required	Hours cooling required	Hours setpoints are met
Jan	744	0	0
Feb	672	0	0
Mar	729	5	10
Apr	681	16	23
May	628	64	52
Jun	483	158	79
Jul	352	308	84
Aug	420	237	87
Sep	528	151	41
Oct	678	31	35
Nov	817	0	2
Dec	744	0	0

Fig. 5 illustrates the monthly heating and cooling energy consumption from the two models. We found that our model building, if located in Denver, will consume more heating load than cooling load, as anticipated from the outdoor air temperature distribution. One major finding from this study is that the energy consumption patterns of buildings, with low or no internal mass, are weather driven, which also supports other studies using different models [7], [8], [14], [17], [20].

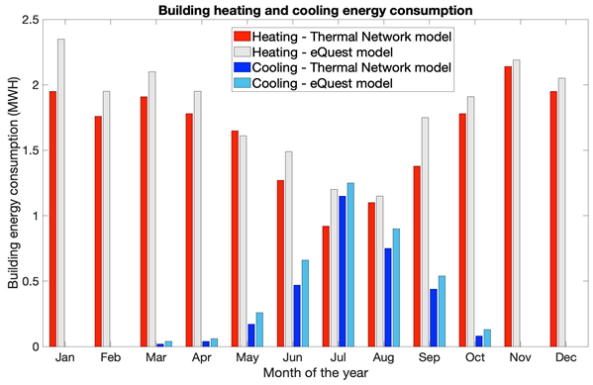

Fig. 5 Monthly building energy consumption comparison

We also studied the effect of the two windows in our model geometry. Our study found that monthly energy consumption of the thermal network model varies from 0.6-9.4% depending on the outdoor air temperature if the south side wall is considered continuous. In most winter months, the two south-facing windows added significant heating loads to the building, whereas the two windows contributed towards the cooling load and actually assisted in meeting the set points in the summer months.

In a comparison of the two models, the thermal network model showed better accuracy in terms of the number of hours set points were not met over the course of the year; 35 hours in the thermal network model and 62 hours in eQuest, which is another important finding from this study and also supports other research utilizing similar mathematical models [12]. It may be noted that number of hours setpoints are not met is an important criteria to be the energy models acceptable by the US Green Building Council for LEED certification. For most of the months, heating and cooling loads from eQuest model are higher than thermal network model results. While the actual reasons are not identified, ASHRAE standards 140 suggests that energy model results from similar programs should not be perceived as better or worse results within a certain range.

Although this kind of mathematical modeling is only used in academic research, because of the significant time required to construct the mathematical model, thermal network models can be effectively utilized to obtain low number of "unmet hours" than commercially available energy modeling tools. Although founded on the same principle, thermal network models are more flexible, if formulated correctly, than commercial energy modeling tools; hence, resolving unmet hours are also often easier. In terms of time step for calculation, thermal network models are not limited, whereas most building energy simulation tools have fixed time steps, however.

We also verified our solar angle calculation in clear sky solar radiation model, manually, using solar angle online calculator, provided by National Renewable Energy Laboratory (NREL), for different time of the day in different seasons.

VII. CONCLUSION

In this study, we utilized the 3R2C thermal network model along with the ASHRAE clear sky solar radiation model to estimate annual building heating and cooling load using historical weather data in MATLAB and compared monthly energy consumption with a "simple-box" energy model. As a future endeavor of this study, we will consider building internal mass, occupancy variation and also transient thermostatic control and analyze the variation in energy consumption.

REFERENCES

[1] Ogunsola, Oluwaseyi T., and Li Song. "Review and evaluation of using RC thermal modeling of cooling load prediction for HVAC system control purpose." In ASME 2012 *International Mechanical Engineering Congress and Exposition*, pp. 735-743. American Society of Mechanical

Engineers, 2012.
[2] Harish, V. S. K. V., and Arun Kumar. "A review on modeling and simulation of building energy systems." *Renewable and Sustainable Energy Reviews* 56 (2016): 1272-1292.
[3] Coakley, Daniel, Paul Raftery, and Marcus Keane. "A review of methods to match building energy simulation models to measured data." *Renewable and sustainable energy reviews* 37 (2014): 123-141.
[4] Li, Xiwang, and Jin Wen. "Review of building energy modeling for control and operation." *Renewable and Sustainable Energy Reviews* 37 (2014): 517-537.
[5] Amasyali, Kadir, and Nora M. El-Gohary. "A review of data-driven building energy consumption prediction studies." *Renewable and Sustainable Energy Reviews* 81 (2018): 1192-1205.
[6] Luo, Qi, and Kartik B. Ariyur. "Building thermal network model and application to temperature regulation." *In Control Applications (CCA), 2010 IEEE International Conference* on, pp. 2190-2195. IEEE, 2010.
[7] Xu, Xinhua, and Shengwei Wang. "Optimal simplified thermal models of building envelope based on frequency domain regression using genetic algorithm." *Energy and Buildings* 39, no. 5 (2007): 525-536.
[8] O'Neill, Zheng, Satish Narayanan, and Rohini Brahme. "Model-based thermal load estimation in buildings." *Proceedings of SimBuild* 4, no. 1 (2010): 474-481.
[9] Rahman, SM Mahbobur. Data driven models applied in building load forecasting for residential and commercial buildings. *The University of Texas at San Antonio*, 2015.
[10] Handbook, A. S. H. R. A. E. "Fundamentals." American Society of Heating, *Refrigerating and Air Conditioning Engineers*, Atlanta 111 (2001).
[11] Ji, Ying, Peng Xu, Pengfei Duan, and Xing Lu. "Estimating hourly cooling load in commercial buildings using a thermal network model and electricity submetering data." *Applied Energy* 169 (2016): 309-323.
[12] Ruya, Elvin, and Godfried Augenbroe. "The Impacts of HVAC Downsizing on Thermal Comfort Hours and Energy Consumption." *Proceedings of SimBuild* 6, no. 1 (2016).
[13] Harb, Hassan, Neven Boyanov, Luis Hernandez, Rita Streblow, and Dirk Müller. "Development and validation of grey-box models for forecasting the thermal response of occupied buildings." *Energy and Buildings* 117 (2016): 199-207.
[14] Rahman, SM Mahbobur, and P. E. Rolando Vega PhD. "Machine Learning Approach Applied in Electricity Load Forecasting: Within Residential Houses Context." *ASHRAE Transactions* 121 (2015): 1V.
[15] Doddi, Harish, Saurav Talukdar, Deepjyoti Deka, and Murti Salapaka. "Data-driven identification of a thermal network in multi-zone building." In 2018 *IEEE Conference on Decision and Control (CDC)*, pp. 7302-7307. IEEE, 2018.
[16] Crawley, Drury B., Jon W. Hand, Michaël Kummert, and Brent T. Griffith. "Contrasting the capabilities of building energy performance simulation programs." *Building and environment* 43, no. 4 (2008): 661-673.
[17] Li, Zhengwei, and Gongsheng Huang. "Re-evaluation of building cooling load prediction models for use in humid subtropical area." *Energy and Buildings* 62 (2013): 442-449.
[18] Dong, Bing, Zhaoxuan Li, SM Mahbobur Rahman, and Rolando Vega. "A hybrid model approach for forecasting future residential electricity consumption." *Energy and Buildings* 117 (2016): 341-351.
[19] Li, Zhaoxuan, S. M. Rahman, Rolando Vega, and Bing Dong. "A hierarchical approach using machine learning methods in solar photovoltaic energy production forecasting." *Energies* 9, no. 1 (2016): 55.
[20] Rahman, SM Mahbobur. Data driven models applied in building load forecasting for residential and commercial buildings. *The University of Texas at San Antonio*, 2015.

S. M. Mahbobur Rahman obtained his BSc in Mechanical Engineering in 2011 from Bangladesh University of Engineering and Technology in Dhaka, Bangladesh. In 2013, he started pursuing MSc in Mechanical Engineering from the University of Texas at San Antonio, in San Antonio, Texas, USA, which he eventually completed in 2015. Later, he started working at Pristine Engineers, Inc., in Rayham, Massachusetts, USA, in 2016 where he is still employed. He is actively involved in building energy modeling research.